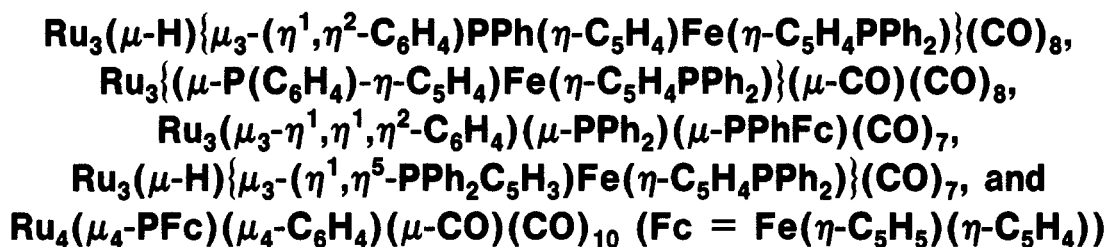


# Cluster Chemistry.<sup>1</sup> Study of the Pyrolysis of Ru<sub>3</sub>(μ-dppf)(CO)<sub>10</sub> (dppf = 1,1'-Bis(diphenylphosphino)ferrocene). X-ray Structures of



Michael I. Bruce,\* Paul A. Humphrey, Omar bin Shawkataly, Michael R. Snow, and  
Edward R. T. Tiekink

Jordan Laboratories, Department of Physical and Inorganic Chemistry, University of Adelaide,  
Adelaide, South Australia 5001, Australia

William R. Cullen\*

Department of Chemistry, University of British Columbia, Vancouver, British Columbia, Canada V6T 1Y6

Received January 26, 1990

Pyrolysis of Ru<sub>3</sub>(CO)<sub>10</sub>(dppf) (cyclohexane, 81 °C, 2 h) gave six major products, of which the title complexes were fully characterized by X-ray crystallographic studies. Structural features include metalated η<sup>1</sup>- and μ-η<sup>1</sup>,η<sup>2</sup>-C<sub>6</sub>H<sub>4</sub> groups, μ<sub>3</sub>-η<sup>1</sup>,η<sup>1</sup>,η<sup>2</sup>- and μ<sub>4</sub>-η<sup>1</sup>,η<sup>1</sup>,η<sup>2</sup>,η<sup>2</sup>-benzyne ligands, and a metalated ferrocene nucleus that further interacts with an Ru<sub>3</sub> cluster via a direct Fe-Ru donor bond. These complexes are formed by reactions involving addition of C-H bonds to clusters, C-H, P-(C<sub>5</sub> ring), and P-(C<sub>6</sub> ring) bond cleavage, and migration of H to C<sub>5</sub> ring carbons to give ferrocenyl (Fe(η-C<sub>5</sub>H<sub>4</sub>)(η-C<sub>5</sub>H<sub>5</sub>)) groups. Crystal data are as follows. Ru<sub>3</sub>(μ-H){μ<sub>3</sub>-(η<sup>1</sup>,η<sup>2</sup>-C<sub>6</sub>H<sub>4</sub>)PPh(η-C<sub>5</sub>H<sub>4</sub>)Fe(η-C<sub>5</sub>H<sub>4</sub>PPh<sub>2</sub>)}(CO)<sub>8</sub>: monoclinic, space group P2<sub>1</sub>/c, a = 17.318 (4) Å, b = 11.635 (2) Å, c = 21.009 (9) Å, β = 110.72 (2)°, V = 3959.4 Å<sup>3</sup>, Z = 4; 3472 data with I ≥ 2.5σ(I) were refined to R = 0.071, R<sub>w</sub> = 0.071. Ru<sub>3</sub>{(μ-(C<sub>6</sub>H<sub>4</sub>)P-η-C<sub>5</sub>H<sub>4</sub>)Fe(η-C<sub>5</sub>H<sub>4</sub>PPh<sub>2</sub>)}(μ-CO)(CO)<sub>8</sub>: monoclinic, space group C2/c, a = 16.050 (4) Å, b = 12.982 (7) Å, c = 35.317 (10) Å, β = 101.29 (2)°, V = 7216.3 Å<sup>3</sup>, Z = 8; 2932 data with I ≥ 2.5σ(I) were refined to R = 0.048, R<sub>w</sub> = 0.039. Ru<sub>3</sub>(μ<sub>3</sub>-η<sup>1</sup>,η<sup>1</sup>,η<sup>2</sup>-C<sub>6</sub>H<sub>4</sub>)(μ-PPh<sub>2</sub>)(μ-PPhFc)(CO)<sub>7</sub>: monoclinic, space group P2<sub>1</sub>/c, a = 11.090 (4) Å, b = 14.337 (3) Å, c = 24.680 (6) Å, β = 94.42 (4)°, V = 3912.4 Å<sup>3</sup>, Z = 4; 5887 data with I ≥ 2.5σ(I) were refined to R = 0.066, R<sub>w</sub> = 0.066. Ru<sub>3</sub>(μ-H){μ-(η<sup>1</sup>,η<sup>5</sup>-PPh<sub>2</sub>C<sub>5</sub>H<sub>3</sub>)Fe(η-C<sub>5</sub>H<sub>4</sub>PPh<sub>2</sub>)}(CO)<sub>8</sub>: monoclinic, space group P2<sub>1</sub>/c, a = 13.166 (5) Å, b = 14.665 (3) Å, c = 22.832 (10) Å, β = 96.59 (3)°, V = 4379.3 Å<sup>3</sup>, Z = 4; 3421 data with I ≥ 2.5σ(I) were refined to R = 0.068, R<sub>w</sub> = 0.072. Ru<sub>4</sub>(μ<sub>4</sub>-PFc)(μ<sub>4</sub>-C<sub>6</sub>H<sub>4</sub>)(μ-CO)(CO)<sub>10</sub>: monoclinic, space group P2<sub>1</sub>/c, a = 14.872 (14) Å, b = 9.008 (6) Å, c = 22.600 (28) Å, β = 91.8 (1)°, V = 3026.1 Å<sup>3</sup>, Z = 4; 1993 data were refined to R = 0.111, R<sub>w</sub> = 0.114, as a result of difficulties with modeling disordered electron density peaks associated with the heavy atoms.

## Introduction

Evidence for the activation of group 15 ligands by coordination to metal cluster carbonyls was first provided in the early 1970s.<sup>2,3</sup> Of particular relevance to the present work, Nyholm and co-workers isolated and characterized nine products from the reaction between Os<sub>3</sub>(CO)<sub>12</sub> and PPh<sub>3</sub> carried out in refluxing xylene.<sup>2</sup> Deeming and co-workers<sup>4</sup> showed that six of these products were derived from Os<sub>3</sub>(CO)<sub>10</sub>(PPh<sub>3</sub>)<sub>2</sub>. The structures of the products indicated that C-H and P-C bond cleavage and, in one case, C-C bond formation had occurred. Thermolysis of an analogous ruthenium system, Ru<sub>3</sub>(CO)<sub>9</sub>(PPh<sub>3</sub>)<sub>3</sub>, afforded mainly complexes containing two ruthenium atoms,

although Ru<sub>3</sub>(μ<sub>3</sub>-C<sub>6</sub>H<sub>4</sub>)(μ-PPh<sub>2</sub>)<sub>2</sub>(CO)<sub>7</sub> (**1a**), containing a cluster-stabilized benzyne ligand, was formed in moderate yield.<sup>5</sup> This type of complex appears to be stable toward further rearrangement, at least under these reaction conditions, and both the ruthenium<sup>6</sup> and osmium<sup>2a,6</sup> complexes **1a** and **1b** have been the subject of X-ray studies, as has the ruthenium-ferrocenylphosphine derivative **1c**.<sup>7</sup>

Many other group 15 ligand derivatives of metal cluster carbonyls have been the subject of similar investigations, and this chemistry has been largely summarized in Garrou's review on P-C bond-cleavage reactions.<sup>8</sup> In the course of these studies, the ease of P-C bond breaking has been established as P-C(sp) > P-C(sp<sup>2</sup>) > P-C(sp<sup>3</sup>). Carty's group,<sup>9</sup> and later ours, have used this feature to

(1) Part 64.

(2) (a) Cullen, W. R.; Harborne, D.; Leingme, B.; Sams, J. R. *Inorg. Chem.* **1970**, *9*, 702. (b) Cullen, W. R. *Adv. Inorg. Chem. Radiochem.* **1972**, *15*, 323. (c) Bradford, C. W.; Nyholm, R. S. *J. Chem. Soc., Dalton Trans.* **1973**, 529.

(3) (a) Bradford, C. W.; Nyholm, R. S.; Gainsford, G. J.; Guss, J. M.; Ireland, P. R.; Mason, R. *J. Chem. Soc., Chem. Commun.* **1972**, 87. (b) Gainsford, G. J.; Guss, J. M.; Ireland, P. R.; Mason, R.; Bradford, C. W.; Nyholm, R. S. *J. Organomet. Chem.* **1972**, *40*, C70.

(4) (a) Deeming, A. J.; Kimber, R. E.; Underhill, M. *J. Chem. Soc., Dalton Trans.* **1973**, 2589. (b) Deeming, A. J.; Underhill, M. *J. Chem. Soc., Dalton Trans.* **1973**, 2727.

(5) Bruce, M. I.; Shaw, G.; Stone, F. G. A. *J. Chem. Soc., Dalton Trans.* **1972**, 2094.

(6) Bruce, M. I.; Guss, J. M.; Mason, R.; Skelton, B. W.; White, A. H. *J. Organomet. Chem.* **1983**, *251*, 261.

(7) Cullen, W. R.; Chacon, S. T.; Bruce, M. I.; Einstein, F. W. B.; Jones, R. H. *Organometallics* **1988**, *7*, 2273.

(8) Garrou, P. E. *Chem. Rev.* **1985**, *85*, 171.

(9) (a) Carty, A. *J. Pure Appl. Chem.* **1982**, *54*, 113. (b) MacLaughlin, S. A.; Taylor, N. J.; Carty, A. *J. Organometallics* **1983**, *2*, 1194. (c) Smith, W. F.; Yule, J.; Taylor, N. J.; Paik, H. N.; Carty, A. *J. Inorg. Chem.* **1977**, *16*, 1593.

advantage to prepare novel polynuclear ruthenium and osmium cluster carbonyls containing unusually reactive acetylide-derived ligands. Central to these studies has been the development of methods of preparations, under mild conditions, of the precursor group 15 ligand complexes from (particularly)  $Ru_3(CO)_{12}$  and  $Os_3(CO)_{12}$ .<sup>11</sup>

The fascinating derivative chemistry of  $Ru_3(\mu-dppm)(CO)_{10}$ ,<sup>12</sup> which on pyrolysis affords  $Ru_3\{\mu_3-PPhCH_2PPh(C_6H_4)\}(CO)_9$  (**2**)<sup>13</sup> or on hydrogenation  $Ru_3(\mu-H)(\mu_3-PPhCH_2PPh_2)(CO)_9$ , for which an extensive chemistry has been developed,<sup>14</sup> is not paralleled by that of  $Ru_3(\mu-dppe)(CO)_{10}$ .<sup>14,15</sup> We considered that a useful extension of these reactions might be achieved using ligands with a different backbone, such as that found in 1,1'-bis(diphenylphosphino)ferrocene (dppf); here, the ferrocene nucleus would not be prone to dehydrogenation and might be expected to produce some kinetically stable intermediates on the way to the final alteration products. In addition, the ferrocenyl nucleus is known to be an excellent electron donor, which might facilitate C-H bond-cleavage reactions by more electron-rich metal cluster atoms.

Before this work was begun, no metal cluster carbonyl complexes containing ferrocenylphosphines had been described, although many mono- and binuclear derivatives are known.<sup>16</sup> Work in our laboratories has since resulted in the identification of several iron and ruthenium cluster carbonyl complexes containing  $PPh_{3-n}Fc_n$  ( $n = 1-3$ ) and  $PBuPhFc$ , as well as the dppf complex used in the present study.<sup>17</sup>

## Results and Discussion

The [ppn][OAc]-catalyzed reaction between  $Ru_3(CO)_{12}$  and dppf affords  $Ru_3(\mu-dppf)(CO)_{10}$  (**3**) in 76% yield in the form of long, dark reddish purple needles of an unusual bis(cyclohexane) solvate. Complex **3** was fully identified by an X-ray structural study and has the familiar triangular  $Ru_3$  core with the dppf ligand bridging one Ru-Ru vector.<sup>17</sup>

The pyrolysis of **3** under mild conditions afforded many products. We have not succeeded in characterizing all of those formed when **3** is heated in refluxing cyclohexane for a short period, preparative TLC revealing at least 18 multihued components of the reaction mixture. However, about one-third of the isolated reaction mass is found in the five complexes **4-8**, which have been fully characterized crystallographically; a sixth, **9**, has been partially identified. Interestingly, two of these were obtained in much higher amounts (about 50% isolated yield) after heating for longer periods, and other experiments (see below) suggest that

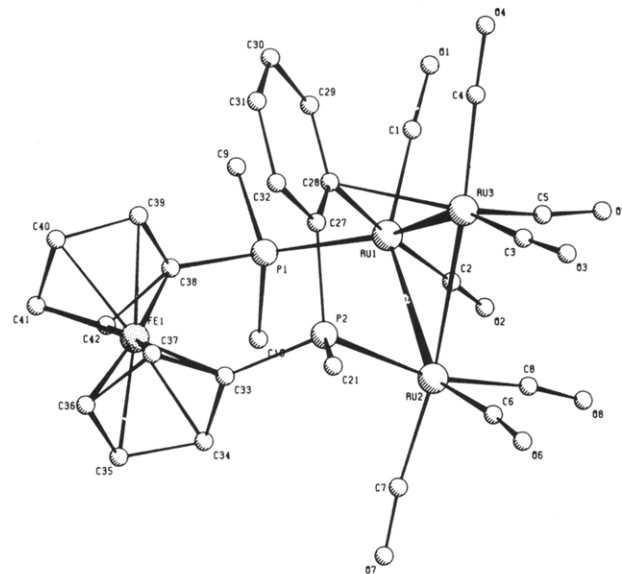
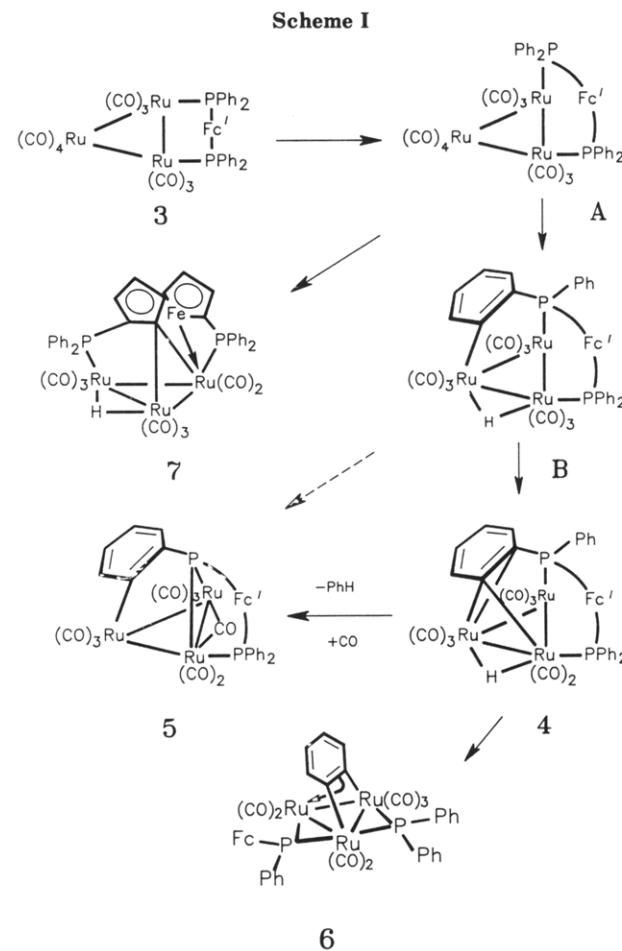


**Figure 1.** ORTEP plot of  $Ru_3(\mu-H)\{\mu_3-PPh(\eta^1, \eta^2-C_6H_4)(\eta-C_5H_4)-Fe(\eta-C_5H_4PPh_2)\}(CO)_8$  (**4**) showing the atom-labeling scheme. Phenyl rings are omitted for clarity.



several of the minor components eventually transform to either complex **6** or **7**. The following is a description of the molecular structures of complexes **4-8**, together with a discussion of possible reaction courses.

The molecular structure of complex **4** is shown in Figure 1. One edge of the triangular  $Ru_3$  core is bridged by the two P atoms ( $Ru(1)-P(1) = 2.330(4)$  Å,  $Ru(2)-P(2) = 2.316(4)$  Å) of a dppf ligand modified by addition of an ortho C-H bond to  $Ru(1)$  ( $Ru(1)-C(28) = 2.12(2)$  Å). The

(10) (a) Bruce, M. I.; Williams, M. L.; Patrick, J. M.; White, A. H. *J. Chem. Soc., Dalton Trans.* **1985**, 1229. (b) Bruce, M. I.; Snow, M. R.; Tiekink, E. R. T.; Williams, M. L. *J. Chem. Soc., Chem. Commun.* **1986**, 701.

(11) (a) Bruce, M. I.; Matison, J. G.; Nicholson, B. K. *J. Organomet. Chem.* **1983**, *247*, 321. (b) Bruce, M. I. *Coord. Chem. Rev.* **1987**, *76*, 1.

(12) Abbreviations used: dppf, 1,1'-bis(diphenylphosphino)ferrocene; Fc, ferrocenyl; ppn, bis(triphenylphosphino)nitrogen(1+); dppm,  $Ph_2PCH_2PPh_2$ ; dppe,  $Ph_2PCH_2CH_2PPh_2$ ;  $Fc'$ ,  $-C_5H_4FeC_5H_4-$ .

(13) (a) Bruce, M. I.; Humphrey, P. A.; Skelton, B. W.; White, A. H.; Williams, M. L. *Aust. J. Chem.* **1985**, *38*, 1301. (b) Lagan, N.; Bonnet, J.-J.; Ibers, J. A. *J. Chem. Soc.* **1985**, *107*, 4484.

(14) (a) Bruce, M. I.; Williams, M. L.; Patrick, J. M.; Skelton, B. W.; White, A. H. *J. Chem. Soc., Dalton Trans.* **1986**, 2557. (b) Bruce, M. I.; Williams, M. L.; Skelton, B. W.; White, A. H. *J. Organomet. Chem.* **1986**, *309*, 157. (c) Bruce, M. I.; Williams, M. L. *J. Organomet. Chem.* **1985**, *288*, C55. (d) Bergonhou, C.; Bonnet, J.-J.; Fompeyrine, P.; Lavigne, G.; Lagan, N.; Mansilla, F. *Organometallics* **1986**, *5*, 60.

(15) Bruce, M. I.; Hambley, T. W.; Nicholson, B. K.; Snow, M. R. *J. Organomet. Chem.* **1982**, *235*, 83.

(16) (a) Cullen, W. R.; Woollins, J. D. *Coord. Chem. Rev.* **1981**, *39*, 1. (b) Hayashi, T.; Kumada, M. *Acc. Chem. Res.* **1982**, *15*, 395.

(17) Chacon, S. T.; Cullen, W. R.; Bruce, M. I.; bin Shawkataly, O.; Einstein, F. W. B.; Jones, R. H.; Willis, A. C. *Can. J. Chem.*, in press.

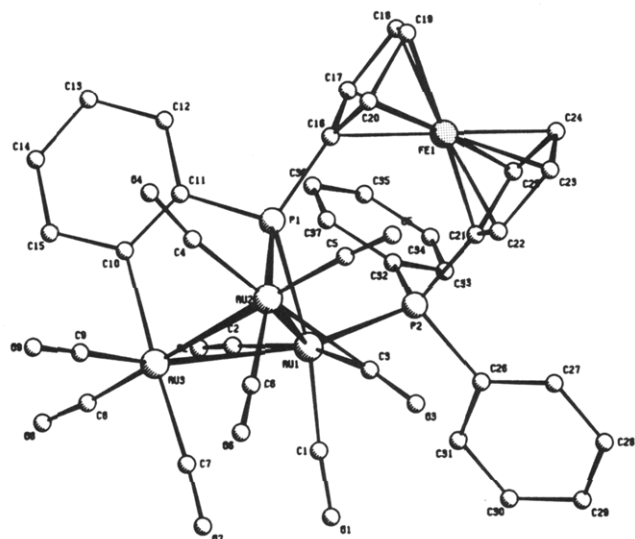
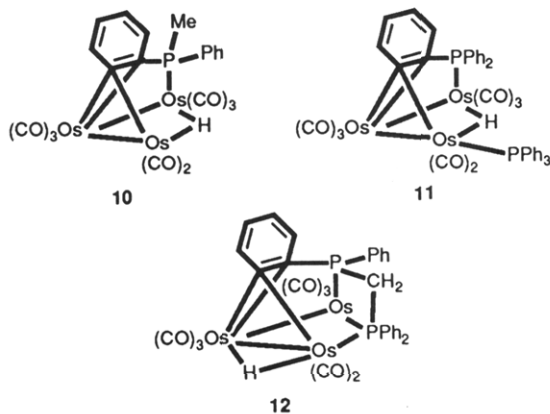


**Figure 2.** ORTEP plot of  $\text{Ru}_3(\mu_3\text{-}\eta^1, \eta^1, \eta^2\text{-C}_6\text{H}_4)\text{Fe}(\eta\text{-C}_5\text{H}_4)\text{Fe}(\eta\text{-C}_5\text{H}_4\text{PPh}_2)(\mu\text{-CO})(\text{CO})_8$  (5) showing the atom-labeling scheme.

metalated  $\text{C}_6$  ring is also attached to Ru(3) by C(27) and C(28) ( $\text{Ru}(3)\text{-C}(27) = 2.49$  (2) Å,  $\text{Ru}(3)\text{-C}(28) = 2.34$  (1) Å), so that the latter bridges the Ru(1)–Ru(3) vector. The  $\text{C}_6$  ring forms an unusual  $\mu\text{-}\eta^1, \eta^2$ -vinyl group in that the carbon bonded to P(2) is involved.

This same bonding is seen in 10 and 11, which are pyrolysis products of  $\text{Os}_3(\text{CO})_{11}(\text{PMePh}_2)$  and  $\text{Os}_3(\text{CO})_{10}(\text{PPh}_3)_2$ , respectively.<sup>18,19</sup> The initial metalation in the



formation of 4 probably takes place at Ru(3) (see also Scheme I), with bond redistribution following subsequent carbonyl displacement. This would be expected for 11 also. Compound 12, an unsaturated product from the pyrolysis of  $\text{Os}_3(\text{CO})_{10}(\mu\text{-dppm})$ ,<sup>21</sup> is an intermediate case with symmetrical binding of the ortho-metalated phenyl group following CO elimination.

The hydride ligands in 4 and 10–12 were not located in the structure determinations; the relatively long Ru(1)–Ru(2) separation (3.000 (2) Å) suggests that the hydrogen atom bridges this bond, so that the same basic structures are found for 4, 10, and 11.

(18) Deeming, A. J.; Kabir, S. E.; Powell, N. I.; Bates, P. A.; Hursthouse, M. B. *J. Chem. Soc., Dalton Trans.* 1987, 1529.

(19) This  $\mu, \eta^2$ -aryl bonding is also found in  $\text{MoRhPt}(\text{CO})_2(\mu\text{-PPh}_2)(\mu, \eta^2\text{-C}_6\text{H}_5)(\text{PPh}_3)_2(\text{C}_6\text{H}_5)$ <sup>20b</sup> and in  $\text{Ru}_2(\mu\text{-H})\{\mu\text{-P}(\text{OC}_6\text{H}_4)(\text{OPh})_2\}\{\mu\text{-OP}(\text{COPh})_2(\text{CO})_3\}$ .<sup>20</sup> In the latter case it is the carbon atoms ortho and meta to the  $\text{P}(\text{OPh})_2$  group that form the  $\eta^2$  attachment.

(20) (a) Farrugia, L. J.; Miles, A. D.; Stone, F. G. A. *J. Chem. Soc., Dalton Trans.* 1984, 2415. (b) Bruce, M. I.; Howard, J.; Nowell, I. W.; Shaw, G.; Woodward, P. *J. Chem. Soc., Chem. Commun.* 1972, 1041.

(21) Clucas, J. A.; Foster, D. F.; Harding, M. M.; Smith, A. K. *J. Chem. Soc., Chem. Commun.* 1984, 949.

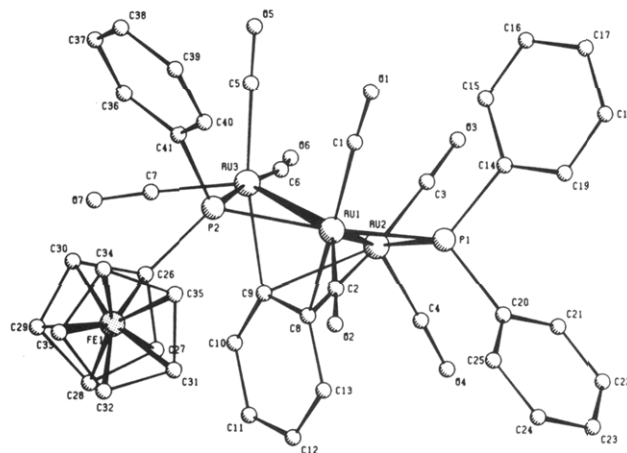


**Figure 3.** ORTEP plot of  $\text{Ru}_3(\mu_3\text{-}\eta^1, \eta^1, \eta^2\text{-C}_6\text{H}_4)(\mu\text{-PPh}_2)(\mu\text{-PPhFc})(\text{CO})_7$  (6) showing the atom-labeling scheme.

The other spectroscopic properties of 4 (IR and  $^1\text{H}$  and  $^{13}\text{C}$  NMR) are consistent with the structure shown in Figure 1 but of themselves did not enable any deductions regarding the molecular structure to be made. In the FAB MS spectrum, recognizable fragmentation of the molecular ion centered on  $m/z$  1083 is by stepwise loss of the eight CO ligands and three Ph groups.

Figure 2 shows a plot of the molecular structure of complex 5. The three ruthenium atoms define an isosceles triangle, with two short Ru–Ru bonds ( $\text{Ru}(1)\text{-Ru}(2) = 2.837$  (1) Å,  $\text{Ru}(2)\text{-Ru}(3) = 2.836$  (1) Å) and one longer bond ( $\text{Ru}(1)\text{-Ru}(3) = 2.869$  (1) Å). The Ru(1)–Ru(2) vector is bridged by the phosphorus atom of a phosphido group ( $\text{Ru}(1)\text{-P}(1) = 2.396$  (3) Å,  $\text{Ru}(2)\text{-P}(1) = 2.335$  (3) Å) and is bridged asymmetrically by a CO ligand ( $\text{Ru}(1)\text{-C}(3) = 1.988$  (13) Å,  $\text{Ru}(2)\text{-C}(3) = 2.415$  (12) Å), which gives rise to the  $\nu(\text{CO})$  absorption at  $1870\text{ cm}^{-1}$ . The phosphido group is formed by loss of a phenyl group from one of the  $\text{PPh}_2$  groups of the original dppf ligand; the remaining  $\text{PPh}_2$  group is attached equatorially to Ru(1) ( $\text{Ru}(1)\text{-P}(2) = 2.354$  (3) Å). A metalated  $\text{C}_6\text{H}_4$  group bridges Ru(3) and P(1) ( $\text{Ru}(3)\text{-C}(10) = 2.15$  (1) Å). Two terminal CO ligands are attached to Ru(1) and three each to Ru(2) and Ru(3). No metal-bonded hydrogen is indicated by the  $^1\text{H}$  NMR spectrum; the complex is electron precise, but there is electron imbalance between Ru(3) (17e) and Ru(1) (19e) that is compensated by the asymmetric  $\mu\text{-CO}$  group mentioned above. Analogous structures have been found for  $\text{Os}_3(\mu_3\text{-C}_6\text{H}_4\text{PMe})(\text{CO})_{10}$ <sup>18</sup> and  $\text{Os}_3(\mu_3\text{-C}_6\text{H}_4\text{PPh})(\mu\text{-Ph})(\mu\text{-PPh}_2)(\text{CO})_9$ ,<sup>2</sup> decomposition products of  $\text{Os}_3(\text{CO})_{11}(\text{PMePh}_2)$  and  $\text{Os}_3(\text{CO})_{10}(\text{PPh}_3)_2$ , respectively. In the former molecule, not surprisingly, the bonding is totally symmetrical.

Complex 6 has the molecular structure shown in Figure 3 and is of the well-known type containing a  $\mu_3$ -benzylidene ligand; previously characterized examples containing ruthenium analogues are known.<sup>7,22</sup> The  $\text{Ru}_3$  triangle has two short Ru–Ru separations ( $\text{Ru}(1)\text{-Ru}(2) = 2.794$  (1) Å,  $\text{Ru}(2)\text{-Ru}(3) = 2.779$  (1) Å) that are bridged respectively by  $\text{PPh}_2$  and  $\text{PPhFc}$  groups ( $\text{Ru}(1)\text{-P}(2) = 2.314$  (2) Å,  $\text{Ru}(3)\text{-P}(2) = 2.378$  (2) Å,  $\text{Ru}(1)\text{-P}(1) = 2.320$  (2) Å,  $\text{Ru}(2)\text{-P}(1) = 2.251$  (2) Å) and a long Ru–Ru bond ( $\text{Ru}(1)\text{-Ru}(3) = 2.938$  (1) Å). The  $\text{C}_6\text{H}_4$  ligand is  $\sigma$ -bonded to Ru(1) and Ru(3) ( $\text{Ru}(1)\text{-C}(8) = 2.138$  Å,  $\text{Ru}(3)\text{-C}(9) = 2.116$  (8) Å) and  $\eta^2$ -bonded to Ru(2) ( $\text{Ru}(2)\text{-C}(8) = 2.313$  (8) Å,  $\text{Ru}(2)\text{-C}(9) = 2.374$  (8) Å). There are two CO ligands each on Ru(1)

(22) Deeming, A. J. *Adv. Organomet. Chem.* 1986, 26, 1.

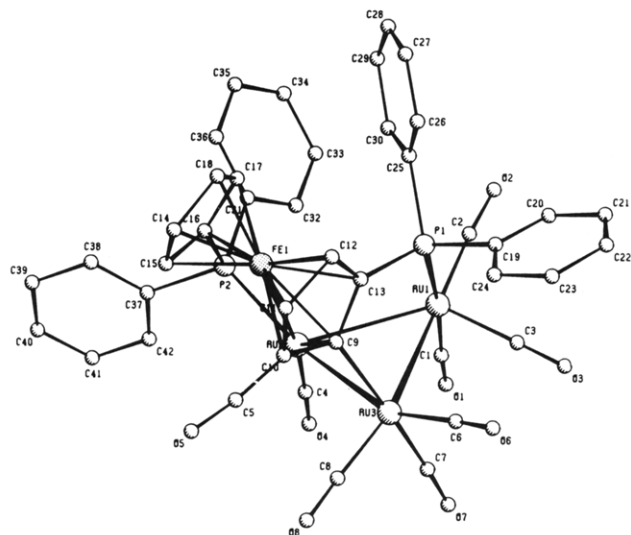


**Figure 4.** ORTEP plot of  $Ru_3(\mu\text{-H})(\mu_3\text{-PPh}_2(\eta^1, \eta^5\text{-C}_5\text{H}_3)\text{Fe}(\eta\text{-C}_5\text{H}_4\text{PPh}_2))(\text{CO})_7$  (7) showing the atom-labeling scheme.

and Ru(2) and three on Ru(3); one of these, CO(6), is bent toward Ru(2) ( $\text{Ru}(3)\text{-C}(6)\text{-O}(6) = 169.8(9)^\circ$ ), as found for **1a** and **1c**. The localized bonding in the benzyne fragment noted in **1c** is apparent in **6**, and generally speaking, the structures of these two molecules are very similar. Although variable-temperature studies were not undertaken, the  $^1\text{H}$  NMR spectrum of **6** in the benzyne region at ambient temperature seems broader than that of **1c**, indicating that the motion of this fragment around the  $Ru_3$  triangle is also facile.

The ferrocenyl group is on the same side of the  $Ru_3$  triangle as the benzyne moiety. There was no indication of the trans isomer in the NMR spectra of this fraction ( $\delta(\text{C}_5\text{H}_5)$  4.3 ppm,  $\delta(\text{C}_5\text{H}_5)$  70.32 ppm). This observation may be of relevance to the mechanism of formation of **6**, as described below. The FAB MS spectrum contains a molecular ion centered on  $m/z$  1055, which fragments by stepwise loss of CO ligands and three Ph groups.

The yellow-green complex **7**, which is formed in the largest amount during the prolonged pyrolysis of **3**, has the unusual structure shown in Figure 4. The  $Ru_3$  core is attached to eight terminal CO ligands and a metalated dppf ligand, which is axially bonded to Ru(1) by one of the  $\text{PPh}_2$  groups ( $\text{Ru}(1)\text{-P}(1) = 2.366(4) \text{ \AA}$ ); the second  $\text{PPh}_2$  group is equatorially bonded to Ru(2) ( $\text{Ru}(2)\text{-P}(2) = 2.306(5) \text{ \AA}$ ). The  $\text{C}_5$  ring bearing P(1) asymmetrically bridges Ru(2)–Ru(3) with C(9) ( $\text{Ru}(2)\text{-C}(9) = 2.45(2) \text{ \AA}$ ,  $\text{Ru}(3)\text{-C}(9) = 2.14(2) \text{ \AA}$ ), this mode of attachment bringing the iron atom within bonding distance, 3.098(3)  $\text{ \AA}$ , of Ru(2).

A few M–Fe (M = Pd, Pt) bonds in ferrocene derivatives have been described;<sup>23</sup> notably the X-ray determination of the structures of  $\text{MFe}(\text{SC}_5\text{H}_4)_2(\text{PPh}_3)$  (M = Pd, Pt),<sup>23a,d</sup> which have dative  $\text{Fe}\rightarrow\text{M}$  bonds of lengths 2.878(1)  $\text{ \AA}$  (Pd) and 2.935(2)  $\text{ \AA}$  (Pt). The short M– $\text{PPh}_3$  bonds (2.241, 2.201(3)  $\text{ \AA}$ ) in these molecules are said to be a consequence of weak donation from the iron. The same may be true for the short P(2)–Ru(2) bond in **7**. The cyclopentadienyl rings in **7** are only slightly opened up (ring plane dihedral angle  $19.7^\circ$ ) as a consequence of the interaction, as are those of the Pd complex. If this Fe–Ru bond is included

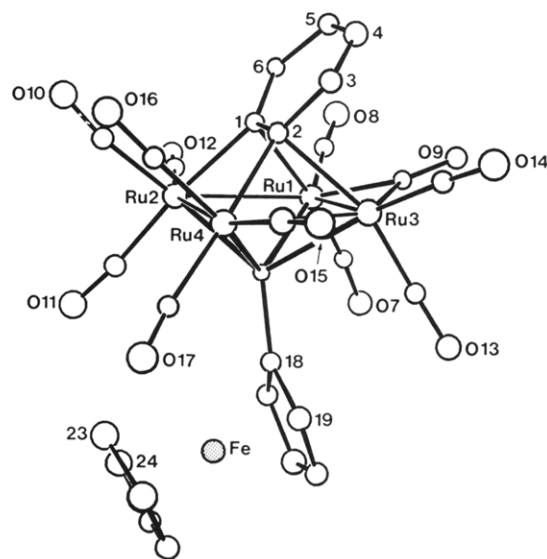
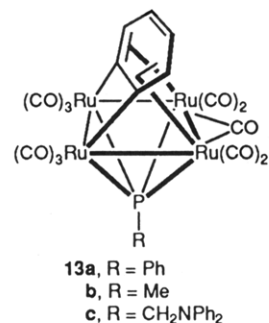


**Figure 5.** ORTEP plot of  $Ru_4(\mu_4\text{-PFc})(\mu_4\text{-C}_6\text{H}_4)(\mu\text{-CO})(\text{CO})_{10}$  (8) showing the atom-labeling scheme. Unlabeled atoms are carbons.

in the electron count, an electron-precise structure is obtained if one hydride from the original ortho metalation remains in the cluster. Individual electron counts at the Ru atoms suggest that the H atom bridges Ru(1)Ru(3) or Ru(2)Ru(3). Evidence for its location is seen in the  $^1\text{H}$  NMR spectrum, which shows a doublet of doublets at  $\delta -12.01$  ppm. This hydrogen atom was not located in the structure determination of **7**; the geometry suggests that it bridges Ru(1)–Ru(2). Ortho metalation of ferrocene derivatives is not unusual.<sup>16a</sup>

The last complex that we have structurally characterized from these reactions is the tetranuclear cluster **8** shown in Figure 5. This structure determination is of limited accuracy (see Experimental Section), but we are confident that the essential structural features have been determined unambiguously. The IR and FAB MS data are consistent with the solid-state structure, which is very similar to those found for molecules **13a–c** obtained by thermal decom-



position of  $Ru_3(\text{CO})_{11}\text{PPh}_2\text{R}$  (R = Ph, Me,  $\text{CH}_2\text{NPh}_2$ ).<sup>24,25</sup> The yellow compound **8** contains an irregular rhombus of four ruthenium atoms, on one face of which is attached a  $\mu_4$ -phosphinidene group, while the opposite side is capped by a  $\mu_4\text{-C}_6\text{H}_4$  ligand. Thus, C(2) is bonded to Ru(4) and Ru(3) ( $\text{Ru}(4)\text{-C}(2) = 2.15(3) \text{ \AA}$ ,  $\text{Ru}(3)\text{-C}(2) = 2.28(3) \text{ \AA}$ ). The corresponding bond lengths in **13c** are 2.117(3) and 2.301(4)  $\text{ \AA}$ , respectively.<sup>24</sup> The  $\text{Ru}(3)\text{-C}(3)$  bond length of 2.61(3)  $\text{ \AA}$  in **8** has its equivalent in **13c** of 2.634(4)  $\text{ \AA}$ . The pattern of bond lengths in the  $\text{C}_6\text{H}_4$  moiety of **13** is quite different from that observed for **1d**. In **13** the ben-

(23) (a) Seyferth, D.; Hames, B. W.; Rucker, T. G.; Cowie, M.; Dickson, R. S. *Organometallics* **1983**, *2*, 472. (b) Sato, M.; Sekino, M.; Akabori, S. *J. Organomet. Chem.* **1988**, *C31*, 344. (c) Sato, M.; Suzuki, K.; Akabori, S. *Chem. Lett.* **1987**, 2239. (d) Akabori, S.; Kumagai, T.; Shirahige, T.; Sato, S.; Kawazoe, K.; Tamura, C.; Sato, M. *Organometallics* **1987**, *6*, 526.

(24) Knox, S. A. R.; Lloyd, B. R.; Orpen, A. G.; Viñas, J. M.; Weber, M. *J. Chem. Soc., Chem. Commun.* **1987**, 1498.

(25) The structure of **8** is incorrectly drawn in ref 7.

zyne ligand shows a localization of multiple bonding, as indicated in the diagram; in **1** the bonds are localized in the opposite sense, as shown. The longest bonds in the benzyne moiety of **1** are those between the carbon atoms that correspond to the  $\eta^2$ -bonded atom in **13**.<sup>17,24</sup> The bridging carbonyl of **8**,  $\nu(\mu\text{-CO})$  1826  $\text{cm}^{-1}$ , spans one of the longer Ru–Ru bonds (Ru(1)–Ru(3) = 2.938 (8) Å, Ru(1)–Ru(2) = 2.886 (6) Å, Ru(2)–Ru(4) = 2.953 (6) Å, Ru(3)–Ru(4) = 2.984 (5) Å). In **13a** the  $\nu(\mu\text{-CO})$  frequency is the same, but this group bridges the shortest Ru–Ru bond, 2.791 (1) Å.<sup>24</sup>

In the structures of **13a** and **13c** the bridging phosphinidene is approximately symmetrically bound to the four ruthenium atoms (e.g. in **13c** the P–Ru distances range from 2.47 to 2.36 Å). In **8** these values are Ru(1)–P(1) = 2.48 (1) Å, Ru(2)–P(1) = 2.38 (1) Å, Ru(3)–P(1) = 2.54 (1) Å and Ru(4)–P(1) = 2.30 (1) Å, indicating a less symmetrical mode. The ferrocenyl group lies below and between the carbonyl groups of Ru(4) and Ru(2); the resulting repulsive interaction bends the ferrocenyl group away from the horizontal.

The spectroscopic properties of **8** include a relatively simple IR  $\nu(\text{CO})$  spectrum, containing five strong terminal  $\nu(\text{CO})$  bands together with the bridging CO absorption at 1826  $\text{cm}^{-1}$  mentioned above. The FAB MS spectrum contains a parent ion centered on  $m/z$  1008 and ions formed by loss of CO, Ph (presumably  $\text{C}_6\text{H}_4$  + cluster-bound H), and Fc groups. The small amount of this complex that was obtained has precluded our recording any NMR spectra.

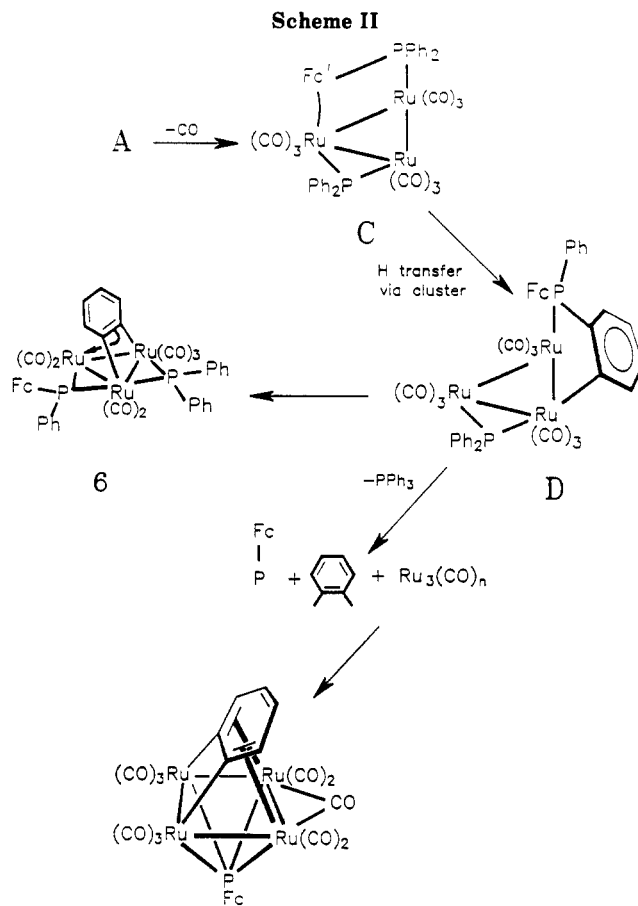
One other complex, orange **9**, has been isolated but did not afford any X-ray-quality crystals. The FAB MS spectrum contains as highest ion one centered on  $m/z$  1160, which corresponds to a formulation such as  $\text{Ru}_4(\text{dppf-Ph})(\text{CO})_{10}$ ; other ions include the stepwise loss of 10 CO and two Ph groups. Several reasonable structures can be proposed at this stage, but we have been unable to distinguish between them.

The results of an FT IR study of the changes occurring as a solution of **3** was heated in refluxing cyclohexane can be summarized as follows. Complex **3** had disappeared after 4.5 h, while **7** began to precipitate after 2 h. The maximum amount of complex **5** is formed after 2 h and, once formed, appears to be relatively stable toward further rearrangement. After 1 h, the amount of **4** increases steadily to maximum after 6 h. Between 7 and 15 h, the IR  $\nu(\text{CO})$  peaks of **6** are the most prominent in the spectra.

Possible routes to these products are outlined in Schemes I and II. The first step, movement of one end of the ligand to an axial site (as in A), seems to be necessary to account for the final geometry found in **4**, **5**, and **6**. The intermediate B results from ortho metalation of one of the P–Ph rings. Similar intermediates have been proposed<sup>12</sup> to account for the products obtained by heating  $\text{Ru}_3(\text{CO})_{10}(\mu\text{-dppm})$ . However, in this case the analogue of B was drawn with two axial phosphorus atoms to account for the elimination of a phenyl group from the unmetallated side of the ligand to produce **2**. Also of relevance to B is the molecule  $\text{Os}_3(\mu\text{-H})(\mu\text{-C}_6\text{H}_4\text{PPh}_2)(\text{CO})_9(\text{PPh}_3)$  of known structure<sup>2</sup> isolated from the thermolysis of  $\text{Os}_3(\text{CO})_{10}(\text{PPh}_3)_2$ ; here the group 15 ligands are both equatorial, there being no need for motion as a consequence of, or prelude to, ortho metalation.

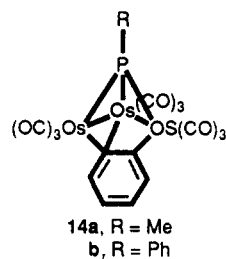
Precedents for the formation of **4** from B are found in **10**–**12** as described above.

The suggestion that **5** arises from **4** via elimination of  $\text{C}_6\text{H}_6$  and addition of CO from solution is based on the observation of Deeming and co-workers<sup>18</sup> that **10** reacts



in this way. In the present case there is the difficulty that the phenyl group in **4** that is lost in forming **5** is pointing away from the metal centers.<sup>26</sup> The alternative path  $\text{B} \rightarrow \text{5}$  directly does not rely on the presence of CO in solution; however, the problem with the orientation of the phenyl group remains.

Compound **10** and its  $\text{PPh}_2$  analogue decompose thermally to the benzyne derivatives containing open  $\text{Os}_3$  clusters (**14**).<sup>18,27</sup> Derivatives related to this are not ob-



tained from the pyrolysis of  $\text{Os}_3(\text{CO})_{10}(\text{PPh}_3)_2$  or, more interestingly,  $\text{Ru}_3(\text{CO})_{11}(\text{PPh}_2\text{R})$ .<sup>24</sup> Decomposition of the last-mentioned compounds affords **13a**–**c**, pentanuclear derivatives, and **1a**.<sup>24,28</sup> Thus, derivatives related to **14** are not expected from the pyrolysis of **3**, whereas tetranuclear species such as **8** could arise by extensive rearrangement of the appropriate fragments. This is the rationale behind the sequence  $\text{A} \rightarrow \text{C} \rightarrow \text{D} \rightarrow \text{8}$  in Scheme II.

The formation of bridging phosphido groups results from the cleavage of a P–Ph bond, presumably via oxidative

(26) This same problem arises in **10**,<sup>18</sup> although it is less serious here because rotation about the Ru–P bond will not be restricted.

(27) Brown, S. C.; Evans, J.; Smart, L. *J. Chem. Soc., Chem. Commun.* 1980, 1021.

(28) Presumably **1a** is formed by pyrolysis of the redistribution product  $\text{Ru}_3(\text{CO})_{10}(\text{PPh}_3)_2$ .

Table I. Crystal Data for 4-8

	4	5	6	7	8
formula	$C_{42}H_{28}FeO_8P_2Ru_3$	$C_{37}H_{28}FeO_8P_2Ru_3$	$C_{41}H_{28}FeO_7P_2Ru_3$	$C_{42}H_{28}FeO_8P_2Ru_3 \cdot CH_3CH_2OH$	$C_{27}H_{13}FeO_{11}PRu_4$
fw	1081.6	1031.6	1053.6	1127.7	1004.5
cryst syst	monoclinic	monoclinic	monoclinic	monoclinic	monoclinic
space group	$P2_1/c$ ( $C_{2h}^5$ , No. 14)	$C2/c$ ( $C_{2h}^6$ , No. 15)	$P2_1/c$ ( $C_{2h}^5$ , No. 14)	$P2_1/c$ ( $C_{2h}^5$ , No. 14)	$P2_1/c$ ( $C_{2h}^5$ , No. 14)
a, Å	17.318 (4)	16.050 (4)	11.090 (4)	13.166 (5)	14.872 (14)
b, Å	11.635 (2)	12.982 (17)	14.337 (3)	14.665 (5)	9.008 (6)
c, Å	21.009 (9)	35.317 (10)	24.680 (6)	22.832 (10)	22.600 (28)
$\beta$ , deg	110.72 (2)	101.29 (2)	94.42 (4)	96.59 (3)	91.8 (1)
V, Å <sup>3</sup>	3959.4	7216.3	3912.4	4379.3	3026.1
Z	4	8	4	4	4
$D_c$ , g cm <sup>-3</sup>	1.815	1.899	1.789	1.709	2.205
F(000)	2128	4032	2072	2232	1920
$\mu$ , cm <sup>-1</sup>	15.60	17.11	15.75	14.13	24.62
max, min transmissn factors	0.9083, 0.6875	0.8651, 0.7485	0.7627, 0.4838	0.9058, 0.6336	0.8317, 0.7042
2 $\theta$ limits, deg	1-22.5	1-22.5	1-25	1-22.5	1-20.0
no. of data collected	9317	7778	9380	6671	4227
no. of unique data	6767	4621	8332	5737	2819
no. of unique data used, $I > 2.5\sigma(I)$	3472	2932	5887	3421	1993
R	0.071	0.048	0.066	0.068	0.110
k	12.15	1.0	5.55	1.28	1.0
g	0.0002	0.0001	0.0005	0.0024	0.0329
$R_w$	0.071	0.039	0.066	0.072	0.114
$\rho_{max}$ , e Å <sup>-3</sup>	0.97	0.78	1.49	1.48	3.24

addition. The Ph group can be lost as PhH or retained as a cluster-bound benzyne. The sequence  $A \rightarrow C \rightarrow D \rightarrow 6$  is one that allows the breaking of a P-(C<sub>5</sub> ring) bond and the formation of a P-Fc moiety. The sequence also accounts for the bridging phosphido groups found in 7. The same sequence of reactions can account for the formation of the many  $\mu_3\text{-}\eta^2$ -benzyne complexes isolated from the pyrolysis of  $M_3(CO)_{10}L_2$  ( $M = Os, Ru$ ) and  $Ru_3(CO)_9L_3$ . Compound 6 could also arise from 4 (Scheme I), and indeed, it is produced when 4 is heated. The latter route may be more attractive because it seems to account for the Fc group in 6 being adjacent to the benzyne fragment. This is a difficulty with the  $D \rightarrow 6$  rearrangement.

Compound 7, which is formed slowly, is a major product; its formation is simply accounted for by ortho metalation of the bridging Fc' group, followed by a second CO displacement as the Fe→Ru bond is formed.<sup>29</sup>

Compounds 4, 5, 6, and 9 have a limited stability in refluxing cyclohexane for 2 h: 6 and 8 are produced from 4, 8 is obtained from 6, and 6 is produced from 9. These products fit into Schemes I and II reasonably well. Somewhat surprisingly, 5, which has lost a phenyl group, decomposes to 6, which necessitates the gain of a phenyl group. The other products from 5 are 8 and 9, which require extensive molecular reorganization.

### Conclusion

The chemistry of the ruthenium cluster complex  $Ru_3(\mu-dppf)(CO)_{10}$  differs substantially from that of  $Ru_3(\mu-dppm)(CO)_{10}$ , mild pyrolysis affording several complexes containing a number of known and novel structural features. These include examples of  $\mu\text{-}\eta^1, \eta^2\text{-}C_6H_4$ ,  $\mu_3\text{-}\eta^2\text{-}C_6H_4$ ,

and  $\mu_4\text{-}\eta^4\text{-}C_6H_4$  ligands and a C-metalated ferrocene derivative that also contains a Fe→Ru bond. Reactions involved include C-H, P-(C<sub>5</sub> ring), and P-(C<sub>6</sub> ring) bond-cleavage reactions and migration of H to C<sub>5</sub> ring carbons, together with cluster disproportionation. In these reactions, formation of benzyne is preferred over that of the still elusive "ferrocene",<sup>7</sup> although the ring metalation found in 7 encourages us further in the search for this ligand. P-(C<sub>5</sub> ring) cleavage is not facile, however.

The reactions outlined in Schemes I and II account for most of the products found from this and related investigations. One noteworthy exception is  $Os_3(\mu\text{-}C_6H_5)(\mu\text{-}PPh_2)(\mu_3\text{-}PPhC_6H_4)(CO)_8$ ,<sup>2</sup> which contains a bridging phenyl group that is probably formed from  $Os_3(CO)_{10}(PPh_3)_2$  via P-Ph bond cleavage without elimination of PhH. Other examples of this type of derivatives are rare in cluster chemistry. Finally, the nonproduction of open cluster derivatives of ruthenium of the type known for osmium, e.g. 14, is noteworthy, considering that some are documented that contain ligands with donor atoms other than P.<sup>22,23</sup>

### Experimental Section

**General Conditions.** All reactions were run under nitrogen; no special precautions were taken to exclude air during workup, since these complexes proved to be stable in air as solids and for short times in solution.

**Instruments:** Perkin-Elmer 683 double-beam spectrometer, NaCl optics (IR); Bruker WP80 spectrometer (<sup>1</sup>H NMR at 80 MHz, <sup>13</sup>C NMR at 20.1 MHz); GEC-Kratos MS3074 mass spectrometer (mass spectra at 70-eV ionizing energy, 4-kV accelerating potential).

FAB mass spectra were obtained on a VG ZAB 2HF instrument equipped with a FAB source. Argon was used as the exciting gas, with source pressures typically 10<sup>-6</sup> mbar; the FAB gun voltage was 7.5 kV and the current 1 mA. The ion accelerating potential was 8 kV. The matrix was 3-nitrobenzyl alcohol. The complexes were made up as ca. 0.5 M solutions in acetone or dichloromethane; a drop was added to a drop of matrix, and the mixture was applied to the FAB probe tip.

**Pyrolysis of  $Ru_3(\mu-dppf)(CO)_{10}$  (3).** (i) **Under Mild Conditions.** A sample of  $Ru_3(\mu-dppf)(CO)_{10}$ <sup>17</sup> (500 mg, 0.44 mmol) was heated in refluxing cyclohexane (200 mL) for 2 h. IR and TLC studies showed that reaction had taken place. Evaporation and preparative TLC (silica gel; petroleum ether/acetone/diethyl ether 60:20:20) gave 18 bands. Bands 1, 2, 5, 6, 7, 8, 11, 12, 14,

(29) Activation of bridging alkyl C-H bonds is found in the thermolysis of  $Os_3(CO)_{10}(\mu-dppm)$ ,<sup>30</sup>  $Ru_3(CO)_{10}(\mu-dppm)$ ,<sup>31</sup> and  $Ru_3(CO)_8(\mu-dppm)$ .<sup>32</sup>

(30) Hodge, S. R.; Johnson, B. F. G.; Lewis, J.; Raithby, P. R. *J. Chem. Soc., Dalton Trans.* 1987, 931.

(31) Clucas, J. A.; Foster, D. F.; Harding, M. M.; Smith, A. K. *J. Chem. Soc., Dalton Trans.* 1987, 277.

(32) Bergounhou, C.; Bonnet, J.-J.; Fompeyrine, P.; Lavigne, G.; Luga, N.; Mansilla, F. *Organometallics* 1986, 5, 60.

(33) Bruce, M. I. In *Comprehensive Organometallic Chemistry*; Wilkinson, G.; Stone, F. G. A.; Abel, E. W., Eds.; Pergamon: Oxford, England, 1982; Vol. 4, pp 843-887.



**Table II. Fractional Atomic Coordinates ( $\times 10^4$ ) for  $\text{Ru}_3(\mu\text{-H})\{\mu_3\text{-PPh}(\eta^1, \eta^2\text{-C}_6\text{H}_4)(\eta\text{-C}_5\text{H}_4)\text{Fe}(\eta\text{-C}_5\text{H}_4\text{PPh}_2)\}(\text{CO})_8$  (4)**

atom	x	y	z
Ru(1)	3006 (1)	1977 (1)	3170 (1)
Ru(2)	1218 (1)	2058 (1)	3017 (1)
Ru(3)	2407 (1)	613 (1)	3951 (1)
Fe(1)	2721 (1)	5636 (2)	3976 (1)
P(1)	3553 (3)	3757 (4)	3045 (2)
P(2)	1690 (2)	3047 (4)	4039 (2)
C(1)	3972 (12)	1105 (15)	3352 (8)
O(1)	4554 (9)	535 (12)	3455 (8)
C(2)	2697 (10)	1597 (13)	2220 (10)
O(2)	2551 (10)	1408 (13)	1659 (7)
C(3)	1606 (12)	-144 (15)	4213 (10)
O(3)	1120 (9)	-695 (12)	4327 (7)
C(4)	3290 (13)	-258 (17)	4591 (10)
O(4)	3815 (9)	-811 (12)	4939 (7)
C(5)	2373 (13)	-229 (17)	3185 (11)
O(5)	2329 (10)	-954 (12)	2801 (8)
C(6)	336 (12)	1354 (17)	3234 (11)
O(6)	-202 (9)	1039 (13)	3360 (9)
C(7)	479 (12)	3186 (16)	2471 (10)
O(7)	-35 (10)	3781 (14)	2169 (9)
C(8)	1035 (12)	1018 (18)	2270 (11)
O(8)	878 (10)	457 (15)	1785 (9)
C(9)	4638 (7)	3718 (9)	3116 (6)
C(10)	5222 (7)	4492 (9)	3519 (6)
C(11)	6025 (7)	4480 (9)	3514 (6)
C(12)	6244 (7)	3693 (9)	3106 (6)
C(13)	5660 (7)	2919 (9)	2703 (6)
C(14)	4857 (7)	2931 (9)	2708 (6)
C(15)	3099 (5)	4456 (11)	2209 (6)
C(16)	3584 (5)	5009 (11)	1896 (6)
C(17)	3211 (5)	5656 (11)	1308 (6)
C(18)	2353 (5)	5751 (11)	1033 (6)
C(19)	1868 (5)	5198 (11)	1347 (6)
C(20)	2241 (5)	4551 (11)	1935 (6)
C(21)	992 (6)	2929 (9)	4527 (6)
C(22)	1032 (6)	2049 (9)	4989 (6)
C(23)	425 (6)	1960 (9)	5281 (6)
C(24)	-222 (6)	2751 (9)	5111 (6)
C(25)	-262 (6)	3631 (9)	4649 (6)
C(26)	345 (6)	3720 (9)	4357 (6)
C(27)	2694 (9)	2495 (15)	4558 (10)
C(28)	3277 (8)	2219 (12)	4230 (9)
C(29)	4090 (10)	2034 (14)	4714 (8)
C(30)	4350 (10)	2126 (15)	5414 (9)
C(31)	3745 (10)	2433 (16)	5684 (8)
C(32)	2925 (11)	2639 (16)	5290 (9)
C(33)	1779 (9)	4588 (14)	4013 (9)
C(34)	1504 (10)	5329 (15)	3421 (10)
C(35)	1634 (11)	6489 (16)	3668 (12)
C(36)	1976 (13)	6496 (19)	4391 (13)
C(37)	2075 (11)	5291 (15)	4618 (10)
C(38)	3569 (9)	4942 (14)	3587 (9)
C(39)	3881 (9)	4922 (13)	4345 (9)
C(40)	3921 (10)	6085 (16)	4574 (10)
C(41)	3609 (11)	6808 (15)	3995 (11)
C(42)	3393 (10)	6128 (14)	3376 (10)

16, 17, and 18 contained trace amounts of unidentified complexes.

Band 3 ( $R_f$  0.82, yellow) gave  $\text{Ru}_4(\mu_4\text{-C}_6\text{H}_4)(\mu_4\text{-PFc})(\mu_2\text{-CO})(\text{CO})_{10}$  (8; 10 mg, 2.3%), recrystallized from *n*-hexane. Crystals suitable for X-ray analysis were grown from slow evaporation of a *n*-hexane solution of 8. IR (cyclohexane):  $\nu(\text{CO})$  2076 vs, 2043 vs, 2014 vs, 1997 w, 1985 vs, 1974 vs, 1826  $\text{m cm}^{-1}$ . FAB MS ( $m/z$ , ion, relative intensity): 1008,  $[\text{M}]^+$ , 2; 924,  $[\text{M} - 3\text{CO}]^+$ , 7; 847,  $[\text{M} - 3\text{CO} - \text{Ph}]^+$ , 39; 791,  $[\text{M} - 5\text{CO} - \text{Ph}]^+$ , 37; 763,  $[\text{M} - 6\text{CO} - \text{Ph}]^+$ , 85; 735,  $[\text{M} - 7\text{CO} - \text{Ph}]^+$ , 62; 707,  $[\text{M} - 8\text{CO} - \text{Ph}]^+$ ; 679,  $[\text{M} - 9\text{CO} - \text{Ph}]^+$ , 100.

Band 4 ( $R_f$  0.80, yellow) was unidentified. IR (cyclohexane):  $\nu(\text{CO})$  2074 vs, 2047 vs, 2037 vs, 2009 s, 2004 m, 1984 s, 1958  $\text{m cm}^{-1}$ .

Band 5 ( $R_f$  0.76, purple) gave  $\text{Ru}_3(\mu_3\text{-C}_6\text{H}_4)(\mu_2\text{-PPh}_2)(\mu_2\text{-PPhFc})(\text{CO})_7$  (6; 45 mg, 9.7%), mp 130 °C dec, recrystallized from  $\text{CH}_2\text{Cl}_2/\text{MeOH}$ . Anal. Calcd for  $\text{C}_{41}\text{H}_{28}\text{FeO}_7\text{P}_2\text{Ru}_3$ : C, 46.74; H, 2.68. Found: C, 47.41; H, 2.84. IR (cyclohexane):  $\nu(\text{CO})$  2055 s, 2015 s, 2006 vs, 1997 s, 1965 m, 1958 m, 1953  $\text{m cm}^{-1}$ .  $^1\text{H NMR}$

**Table III. Fractional Atomic Coordinates ( $\times 10^5$  for Ru,  $\times 10^4$  for Other Atoms) for  $\text{Ru}_3\{\mu\text{-P}(\text{C}_6\text{H}_4)(\eta\text{-C}_5\text{H}_4)\text{Fe}(\eta\text{-C}_5\text{H}_4\text{PPh}_2)\}(\mu\text{-CO})(\text{CO})_8$  (5)**

atom	x	y	z
Ru(1)	29258 (7)	41087 (9)	10765 (3)
Ru(2)	38370 (7)	41620 (9)	18504 (3)
Ru(3)	26316 (8)	25727 (9)	16194 (3)
Fe(1)	2978 (1)	7473 (2)	1300 (1)
P(1)	2592 (2)	5069 (3)	1607 (1)
P(2)	2699 (2)	5505 (3)	642 (1)
C(1)	3222 (10)	3139 (12)	732 (5)
O(1)	3418 (9)	2566 (10)	508 (4)
C(2)	1794 (10)	3498 (12)	966 (4)
O(2)	1137 (7)	3216 (9)	828 (4)
C(3)	4167 (10)	4353 (11)	1218 (4)
O(3)	4842 (7)	4396 (9)	1148 (3)
C(4)	3537 (9)	4116 (13)	2331 (5)
O(4)	3328 (8)	4197 (11)	2629 (3)
C(5)	4649 (10)	5256 (13)	1981 (4)
O(5)	5164 (8)	5866 (9)	2076 (4)
C(6)	4702 (11)	3072 (12)	1946 (5)
O(6)	5192 (8)	2494 (10)	2029 (4)
C(7)	3495 (11)	1781 (13)	1425 (5)
O(7)	3980 (9)	1278 (10)	1314 (4)
C(8)	1775 (12)	1608 (13)	1421 (5)
O(8)	1228 (9)	1054 (10)	1332 (4)
C(9)	2841 (11)	1976 (13)	2116 (6)
O(9)	2951 (9)	1604 (11)	2412 (4)
C(10)	1676 (8)	3483 (10)	1812 (4)
C(11)	1691 (9)	4565 (10)	1775 (4)
C(12)	1051 (9)	5195 (13)	1877 (5)
C(13)	399 (10)	4751 (13)	2031 (5)
C(14)	403 (11)	3665 (18)	2056 (5)
C(15)	1026 (11)	3039 (14)	1952 (5)
C(16)	2521 (9)	6426 (11)	1638 (5)
C(17)	1841 (9)	7117 (11)	1443 (4)
C(18)	2093 (10)	8140 (12)	1566 (5)
C(19)	2873 (9)	8136 (12)	1825 (5)
C(20)	3170 (10)	7111 (11)	1874 (5)
C(21)	3120 (8)	6730 (10)	812 (4)
C(22)	3935 (10)	6922 (12)	1061 (5)
C(23)	4069 (9)	7998 (12)	1116 (5)
C(24)	3321 (10)	8473 (13)	923 (5)
C(25)	2740 (9)	7724 (11)	720 (4)
C(26)	3155 (6)	5305 (6)	214 (2)
C(27)	3831 (6)	5911 (6)	148 (2)
C(28)	4170 (6)	5755 (6)	-182 (2)
C(29)	3833 (6)	4994 (6)	-447 (2)
C(30)	3157 (6)	4389 (6)	-382 (2)
C(31)	2818 (6)	4544 (6)	-51 (2)
C(32)	1586 (5)	5813 (7)	439 (2)
C(33)	1367 (5)	6219 (7)	67 (2)
C(34)	525 (5)	6482 (7)	-84 (2)
C(35)	-98 (5)	6339 (7)	136 (2)
C(36)	121 (5)	5934 (7)	508 (2)
C(37)	964 (5)	5670 (7)	659 (2)

( $\delta$ ,  $\text{CDCl}_3$ ): 3.8–4.6 (m, 9 H,  $\text{C}_6\text{H}_4$ ), 6.3–7.8 (m, 19 H, Ph +  $\text{C}_6\text{H}_4$ ). FAB MA ( $m/z$ , ion, relative intensity): 1055,  $[\text{M}]^+$ , 16; 999,  $[\text{M} - 2\text{CO}]^+$ , 8; 971,  $[\text{M} - 3\text{CO}]^+$ , 21; 943,  $[\text{M} - 4\text{CO}]^+$ , 32; 915,  $[\text{M} - 5\text{CO}]^+$ , 47; 887,  $[\text{M} - 6\text{CO}]^+$ , 32; 859,  $[\text{M} - 7\text{CO}]^+$ , 89; 782,  $[\text{M} - 7\text{CO} - \text{Ph}]^+$ , 71; 705,  $[\text{M} - 7\text{CO} - 2\text{Ph}]^+$ , 79; 628,  $[\text{M} - 7\text{CO} - 3\text{Ph}]^+$ , 100.

Band 6 ( $R_f$  0.61, yellow) was unidentified. IR (cyclohexane):  $\nu(\text{CO})$  2062 m, br, 2017 s, 2002 m, 1973  $\text{s cm}^{-1}$ .

Band 9 ( $R_f$  0.54, orange) contained complex 9 (10 mg, 2%), recrystallized from hexane. IR (cyclohexane):  $\nu(\text{CO})$  2063 w, 2033 vs, 2021 vs, 2007 w, 1989 m, 1972 w, 1953  $\text{w cm}^{-1}$ . FAB MS ( $m/z$ , ion, relative intensity): 1160,  $[\text{M}]^+$ , 32; 1132,  $[\text{M} - \text{CO}]^+$ , 6; 1104,  $[\text{M} - 2\text{CO}]^+$ , 6; 1076,  $[\text{M} - 3\text{CO}]^+$ , 95; 1048,  $[\text{M} - 4\text{CO}]^+$ , 45; 1020,  $[\text{M} - 5\text{CO}]^+$ , 59; 992,  $[\text{M} - 6\text{CO}]^+$ , 100; 964,  $[\text{M} - 7\text{CO}]^+$ , 27; 936,  $[\text{M} - 8\text{CO}]^+$ , 41; 908,  $[\text{M} - 9\text{CO}]^+$ , 32; 880,  $[\text{M} - 10\text{CO}]^+$ , 95; 803,  $[\text{M} - 10\text{CO} - \text{Ph}]^+$ , 73; 726,  $[\text{M} - 10\text{CO} - 2\text{Ph}]^+$ , 55.

Band 10 ( $R_f$  0.48, red) gave  $\text{Ru}_3\{\mu_3\text{-}(\text{C}_6\text{H}_4)\text{PFc}(\text{C}_6\text{H}_4)\}(\mu_2\text{-CO})(\text{CO})_8$  (5; 20 mg, 4.4%), mp 111–113 °C dec, recrystallized from  $\text{CH}_2\text{Cl}_2/\text{MeOH}$ . Crystals suitable for X-ray analysis were grown from solvent diffusion of  $\text{CH}_2\text{Cl}_2/\text{MeOH}$ . Anal. Calcd for  $\text{C}_{37}\text{H}_{22}\text{FeO}_9\text{P}_2\text{Ru}_3$ : C, 43.08; H, 2.15. Found: C, 43.08; H, 2.30.

**Table IV. Fractional Atomic Coordinates ( $\times 10^5$  for Ru,  $\times 10^4$  for Other Atoms) for  $Ru_3(\mu_3-\eta^1, \eta^1, \eta^2-C_6H_4)(\mu-PPh_2)(\mu-PPhFc)(CO)_7$  (6)**

atom	x	y	z
Ru(1)	31070 (5)	63882 (4)	24498 (3)
Ru(2)	20649 (6)	75911 (4)	16553 (3)
Ru(3)	25954 (5)	83524 (4)	26813 (3)
Fe(1)	1479 (1)	5723 (1)	4211 (1)
P(1)	3135 (2)	6291 (1)	1513 (1)
P(2)	2925 (2)	7074 (1)	3288 (1)
C(1)	4851 (7)	6359 (7)	2535 (4)
O(1)	5876 (6)	6321 (7)	2564 (3)
C(2)	2824 (7)	5140 (6)	2646 (4)
O(2)	2632 (7)	4402 (4)	2775 (3)
C(3)	2872 (11)	8340 (8)	1198 (5)
O(3)	3389 (10)	8828 (6)	912 (4)
C(4)	790 (9)	7422 (7)	1115 (4)
O(4)	6 (7)	7272 (7)	798 (3)
C(5)	4270 (8)	8754 (6)	2821 (5)
O(5)	5245 (7)	8954 (7)	2900 (4)
C(6)	2254 (9)	9324 (6)	2138 (4)
O(6)	2065 (9)	9972 (5)	1888 (3)
C(7)	1889 (8)	8995 (6)	3258 (4)
O(7)	1431 (7)	9341 (5)	3594 (3)
C(8)	1224 (7)	6692 (5)	2307 (3)
C(9)	974 (7)	7631 (5)	2446 (3)
C(10)	-234 (7)	7946 (6)	2437 (4)
C(11)	-1175 (7)	7323 (7)	2302 (4)
C(12)	-944 (7)	6424 (6)	2156 (4)
C(13)	224 (7)	6096 (6)	2143 (4)
C(14)	4599 (5)	6367 (3)	1215 (3)
C(15)	5335 (5)	7143 (3)	1327 (3)
C(16)	6499 (5)	7168 (3)	1149 (3)
C(17)	6927 (5)	6418 (3)	860 (3)
C(18)	6191 (5)	5641 (3)	748 (3)
C(19)	5027 (5)	5616 (3)	925 (3)
C(20)	2377 (5)	5395 (3)	1087 (2)
C(21)	2104 (5)	5583 (3)	537 (2)
C(22)	1517 (5)	4913 (3)	202 (2)
C(23)	1204 (5)	4055 (3)	418 (2)
C(24)	1477 (5)	3867 (3)	968 (2)
C(25)	2064 (5)	4537 (3)	1303 (2)
C(26)	1720 (7)	6848 (5)	3722 (4)
C(27)	601 (8)	6401 (7)	3567 (4)
C(28)	-114 (9)	6390 (8)	4024 (5)
C(29)	558 (11)	6850 (7)	4460 (5)
C(30)	1705 (10)	7112 (6)	4279 (4)
C(31)	1609 (10)	4359 (7)	4002 (6)
C(32)	1038 (12)	4463 (8)	4490 (7)
C(33)	1818 (13)	4918 (10)	4885 (6)
C(34)	2928 (10)	5085 (8)	4633 (5)
C(35)	2779 (10)	4742 (7)	4100 (5)
C(36)	4463 (7)	7933 (4)	4104 (3)
C(37)	5442 (7)	7954 (4)	4494 (3)
C(38)	6218 (7)	7189 (4)	4556 (3)
C(39)	6014 (7)	6403 (4)	4228 (3)
C(40)	5035 (7)	6382 (4)	3838 (3)
C(41)	4259 (7)	7147 (4)	3776 (3)

IR (cyclohexane): 1076 vs, 2038 vs, 2024 vs, 2007 s, 1999 sh, 1983 sh, 1978 s, 1865 w  $cm^{-1}$ .  $^1H$  NMR ( $\delta$ ,  $CDCl_3$ ): 3.4–4.7 (m, 9 H,  $C_6H_4$ , 7.1–7.6 (m, 14 H, Ph +  $C_6H_4$ ). FAB MS ( $m/z$ , ion, relative intensity): 1033,  $[M]^+$ , 22; 977,  $[M - 2CO]^+$ , 36; 949,  $[M - 3CO]^+$ , 29; 921,  $[M - 4CO]^+$ , 18; 893,  $[M - 5CO]^+$ , 65; 865,  $[M - 6CO]^+$ , 100; 837,  $[M - 7CO]^+$ , 39; 809,  $[M - 8CO]^+$ , 26; 781,  $[M - 8CO]^+$ , 68; 704  $[M - 8CO - Ph]^+$ , 43; 627,  $[M - 8CO - 2Ph]^+$ , 42.

Band 13 ( $R_f$  0.34, orange) was  $Ru_3(\mu-H)(\mu_3-(C_6H_4)-PPhFcPPh_2)(CO)_8$  (4) (60 mg, 12.6%), mp 180 °C dec, recrystallized from  $CH_2Cl_2/MeOH$ . Crystals suitable for X-ray analysis were grown from solvent diffusion of  $CH_2Cl_2/MeOH$ . Anal. Calcd for  $C_{42}H_{28}FeO_8P_2Ru_3$ : C, 46.68; H, 2.61. Found: C, 46.46; H, 2.86. IR (cyclohexane):  $\nu(CO)$  2067 vs, 2027 vs, 2015 vs, 2000 m, 1981 s, 1966 m, 1950  $cm^{-1}$ .  $^1H$  NMR ( $\delta$ ,  $CDCl_3$ ): -16.7 (d, d, 1 H, RuH), 3.2–4.7 (m, 8 H,  $C_6H_4$ ), 7.1–7.7 (m, 19 H, Ph +  $C_6H_4$ ). FAB MS ( $m/z$ , ion, relative intensity): 1083,  $[M]^+$ , 44; 1055,  $[M - CO]^+$ , 31; 1027,  $[M - 2CO]^+$ , 46; 999,  $[M - 3CO]^+$ , 47; 971,  $[M - 4CO]^+$ , 63; 943  $[M - 5CO]^+$ , 100; 915,  $[M - 6CO]^+$ , 89; 887,  $[M - 7CO]^+$ ,

**Table V. Fractional Atomic Coordinates ( $\times 10^4$ ) for  $Ru_3(\mu-H)(\mu_3-PPh_2)(\eta^1, \eta^5-C_5H_3)Fe(\eta-C_5H_4PPh_2)(CO)_7$  (7)**

atom	x	y	z
Ru(1)	1090 (1)	1331 (1)	5584 (1)
Ru(2)	3280 (1)	1996 (1)	5843 (1)
Ru(3)	2029 (1)	2736 (1)	4953 (1)
Fe(1)	2909 (2)	3545 (2)	6716 (1)
P(1)	600 (3)	2532 (3)	6184 (2)
P(2)	4066 (3)	1572 (3)	6757 (2)
C(1)	1597 (13)	407 (13)	5100 (9)
O(1)	1873 (11)	-191 (10)	4824 (6)
C(2)	468 (15)	444 (13)	6015 (9)
O(2)	3 (12)	-111 (10)	6250 (7)
C(3)	24 (15)	1629 (12)	4972 (9)
O(3)	-612 (11)	1758 (9)	4612 (6)
C(4)	3697 (13)	1082 (16)	5378 (10)
O(4)	4001 (11)	532 (12)	5094 (8)
C(5)	4387 (13)	2679 (13)	5688 (9)
O(5)	5096 (11)	3129 (11)	5608 (8)
C(6)	856 (14)	3442 (12)	4673 (8)
O(6)	199 (11)	3878 (9)	4491 (6)
C(7)	2038 (16)	1927 (15)	4313 (9)
O(7)	2031 (14)	1478 (11)	3904 (7)
C(8)	2998 (16)	3464 (14)	4648 (10)
O(8)	3574 (12)	3941 (12)	4457 (8)
C(9)	2264 (13)	3401 (11)	5791 (7)
C(10)	2851 (13)	4246 (12)	5928 (8)
C(11)	2400 (14)	4746 (12)	6344 (9)
C(12)	1586 (14)	4275 (11)	6522 (7)
C(13)	1504 (11)	3426 (11)	6216 (7)
C(14)	3871 (15)	4110 (14)	7383 (9)
C(15)	4405 (14)	3435 (13)	7097 (8)
C(16)	3889 (12)	2591 (12)	7180 (7)
C(17)	3026 (13)	2777 (12)	7483 (7)
C(18)	3023 (15)	3695 (13)	7618 (7)
C(19)	-629 (8)	3042 (6)	5919 (5)
C(20)	-1490 (8)	2486 (6)	5912 (5)
C(21)	-2452 (8)	2824 (6)	5699 (5)
C(22)	-2553 (8)	3718 (6)	5492 (5)
C(23)	-1693 (8)	4275 (6)	5499 (5)
C(24)	-731 (8)	3937 (6)	5712 (5)
C(25)	404 (10)	2286 (7)	6955 (6)
C(26)	-118 (10)	2928 (7)	7257 (6)
C(27)	-263 (10)	2779 (7)	7846 (6)
C(28)	115 (10)	1988 (7)	8132 (6)
C(29)	638 (10)	1345 (7)	7829 (6)
C(30)	782 (10)	1494 (7)	7241 (6)
C(31)	3599 (9)	649 (8)	7189 (3)
C(32)	3100 (9)	-78 (8)	6886 (3)
C(33)	2741 (9)	-807 (8)	7197 (3)
C(34)	2883 (9)	-808 (8)	7812 (3)
C(35)	3382 (9)	-81 (8)	8116 (3)
C(36)	3741 (9)	648 (8)	7804 (3)
C(37)	5446 (9)	1388 (8)	6847 (5)
C(38)	6067 (9)	1722 (8)	7336 (5)
C(39)	7114 (9)	1543 (8)	7401 (5)
C(40)	7541 (9)	1028 (8)	6977 (5)
C(41)	6920 (9)	694 (8)	6488 (5)
C(42)	5873 (9)	874 (8)	6423 (5)
C(43)	4951 (15)	1825 (14)	3768 (9)
C(44)	5770 (31)	2263 (48)	4173 (32)
O(9)	6772 (25)	2502 (21)	4023 (14)

53; 859,  $[M - 8CO]^+$ , 88; 782  $[M - 8CO - Ph]^+$ , 89; 705,  $[M - 8CO - 2Ph]^+$ , 97.

Band 15 ( $R_f$  0.27, yellowish green) was complex 7 (20 mg, 4.1%), mp 210 °C, recrystallized from acetone/*n*-hexane. Crystals suitable for X-ray analysis separated from solution when complex 3 was pyrolyzed in cyclohexane for 18 h (see (ii) below). Anal. Calcd for  $C_{42}H_{28}FeO_8P_2Ru_3$ : C, 46.62; H, 2.59. Found: C, 45.92; H, 2.71. IR (cyclohexane):  $\nu(CO)$  2076 s, 2038 vs, 2024 vs, 2007 s, 1999 sh, 1983 sh, 1978 s  $cm^{-1}$ . IR ( $CH_2Cl_2$ ): 2060 vs, 2018 vs, 1999 vs, 1946 m (br)  $cm^{-1}$ .  $^1H$  NMR ( $\delta$ ,  $CDCl_3$ ): -16.47 (d, d,  $J(HP) = 6, 12$  Hz, 1 H, RuH), 2.16, 3.26, 3.57, 4.60, 5.15, 5.43 (m, H,  $C_5H_4 + C_5H_3$ ), 6.6–8.15 (m, H, Ph +  $C_6H_4$ ).  $^{31}P$  NMR ( $\delta$ ,  $CH_2Cl_2$ ): 4.56, 35.38. FAB MS ( $m/z$ , ion, relative intensity): 1080,  $[M]^+$ , 24; 1052,  $[M - CO]^+$ , 29; 1024,  $[M - 2CO]^+$ , 25; 996,  $[M - 3CO]^+$ , 32; 968,  $[M - 4CO]^+$ , 60; 940,  $[M - 5CO]^+$ , 59; 912,  $[M -$



**Table VI. Fractional Atomic Coordinates ( $\times 10^4$ ) for  $\text{Ru}_4(\mu_4\text{-PFC})(\mu_4\text{-C}_6\text{H}_4)(\mu\text{-CO})(\text{CO})_{10}$  (8)**

atom	x	y	z
Ru(1)	6483 (2)	1143 (2)	1160 (1)
Ru(2)	6393 (2)	-1991 (2)	1403 (1)
Ru(3)	8387 (2)	1131 (2)	1312 (1)
Ru(4)	8397 (2)	-2021 (2)	1568 (1)
Fe(1)	7740 (3)	-2659 (4)	-576 (2)
P(1)	7497 (5)	-879 (6)	827 (3)
C(1)	6824 (17)	-287 (30)	1982 (12)
C(2)	7810 (17)	-321 (29)	2059 (12)
C(3)	8251 (18)	807 (34)	2461 (13)
C(4)	7660 (22)	1775 (37)	2732 (15)
C(5)	6822 (18)	1793 (30)	2690 (12)
C(6)	6308 (17)	786 (30)	2322 (12)
C(7)	6278 (19)	1790 (30)	416 (12)
O(7)	6103 (15)	2258 (26)	-69 (11)
C(8)	5479 (20)	2219 (35)	1339 (14)
O(8)	4850 (19)	2922 (33)	1475 (13)
C(9)	7434 (15)	2684 (32)	1333 (11)
O(9)	7413 (12)	4051 (25)	1382 (9)
C(10)	6284 (18)	-3344 (35)	2021 (13)
O(10)	6124 (15)	-3972 (26)	2452 (10)
C(11)	6127 (18)	-3467 (35)	858 (12)
O(11)	5821 (16)	-4440 (29)	521 (11)
C(12)	5171 (19)	-1287 (31)	1365 (12)
O(12)	4427 (14)	-967 (22)	1386 (9)
C(13)	8800 (19)	1715 (31)	585 (15)
O(13)	9078 (14)	2233 (24)	167 (10)
C(14)	9349 (22)	2237 (35)	1689 (14)
O(14)	9959 (17)	2898 (29)	1835 (11)
C(15)	9604 (21)	-1460 (37)	1758 (14)
O(15)	10337 (16)	-1173 (25)	1838 (10)
C(16)	8319 (18)	-3244 (32)	2208 (13)
O(16)	8242 (15)	-4016 (27)	2628 (11)
C(17)	8784 (15)	-3550 (29)	1073 (11)
O(17)	9135 (17)	-4525 (30)	807 (12)
C(18)	7669 (18)	-1020 (31)	65 (13)
C(19)	8520 (21)	-952 (35)	-248 (14)
C(20)	8408 (19)	-853 (32)	-826 (13)
C(21)	7422 (19)	-709 (34)	-975 (13)
C(22)	6985 (18)	-809 (33)	-447 (12)
C(23)	7614 (24)	-4768 (43)	-237 (17)
C(24)	6866 (21)	-4410 (38)	-701 (15)
C(25)	7277 (19)	-4108 (33)	-1197 (12)
C(26)	8275 (20)	-4233 (34)	-1121 (14)
C(27)	8451 (24)	-4596 (41)	-559 (17)

6CO)<sup>+</sup>, 100; 884, [M - 7CO]<sup>+</sup>, 42; 856, [M - 8CO]<sup>+</sup>, 49; 779, [M - 8CO - Ph]<sup>+</sup>, 59; 715, [M - 8CO - 2Ph]<sup>+</sup>, 71; 674, [M - 8CO - 3Ph]<sup>+</sup>, 51.

(ii) **Under Vigorous Conditions.** When a solution of **3** (400 mg, 0.35 mmol) was pyrolyzed in cyclohexane for 18 h, preparative TLC still produced 18 bands. However, the only products in significant amount were complexes **6** (50 mg, 14%) and **7** (150 mg, 40%). The maximum amounts of complex **7** were obtained after heating for 24 h (55–67%).

**Pyrolyses of Individual Complexes Isolated from the Above Reactions.** Pure samples of complexes **4–6** and **9** were heated in refluxing cyclohexane for 2 h, and the resulting mixture was separated by preparative TLC (3/1/1 light petroleum ether/acetone/diethyl ether), with comparison spots of the complexes being run on the same plates. The results were as follows: (a) complex **4**, 10 products, including complexes **4**, **6**, and **8**; (b) complex **5**, 11 products, including complexes **5**, **6**, **8**, and **9**; (c) complex **6**, 4 products, including complexes **6** and **8**; (d) complex **9**, 4 products, including complexes **6** and **9**.

**Crystallography.** Intensity data for each of the crystals were measured at room temperature on an Enraf-Nonius CAD4F diffractometer fitted with Mo K $\alpha$  (graphite monochromatized) radiation,  $\lambda = 0.71073$  Å, with the use of the  $\omega:2\theta$  scan technique. The net intensity values of three standard reflections were monitored after every 3600 s of X-ray exposure time, and these indicated that no decomposition of any of the samples occurred during their respective data collections. Corrections were routinely applied for Lorentz and polarization effects as well as for absorption by employing an analytical procedure.<sup>34</sup> Relevant crystal

**Table VII. Selected Bond Lengths (Å) and Angles (deg) for 4**

Distances			
Ru(1)–Ru(2)	3.000 (2)	Ru(1)–Ru(3)	2.736 (2)
Ru(2)–Ru(3)	2.838 (2)	Ru(1)–P(1)	2.330 (4)
Ru(2)–P(2)	2.316 (4)	Ru(1)–C(28)	2.13 (2)
Ru(3)–C(27)	2.49 (2)	Ru(3)–C(28)	2.34 (1)
P(1)–C(27)	1.81 (2)		
Angles			
Ru(1)–C(28)–C(27)	127 (1)	Ru(2)–P(2)–C(27)	109.3 (6)
P(2)–C(27)–C(28)	118 (1)	Ru(1)–C(28)–Ru(3)	75.4 (4)

**Table VIII. Selected Bond Lengths (Å) and Angles (deg) for 5**

Distances			
Ru(1)–Ru(2)	2.837 (1)	Ru(1)–Ru(3)	2.869 (1)
Ru(2)–Ru(3)	2.836 (1)	Ru(1)–P(1)	2.396 (3)
Ru(2)–P(1)	2.335 (3)	Ru(1)–P(2)	2.354 (3)
Ru(1)–C(3)	1.99 (1)	Ru(2)–C(3)	2.42 (1)
Ru(3)–C(10)	2.15 (1)	P(1)–C(11)	1.80 (1)
P(1)–C(16)	1.79 (1)		
Angles			
Ru(1)–P(1)–Ru(2)	73.7 (1)	Ru(1)–C(3)–Ru(2)	79.6 (4)
Ru(1)–C(3)–O(3)	153 (1)	Ru(2)–C(3)–O(3)	126 (1)
Ru(3)–C(10)–C(11)	120.2 (9)	Ru(3)–C(10)–C(15)	122.3 (9)

**Table IX. Selected Bond Lengths (Å) and Angles (deg) for 6**

Distances			
Ru(1)–Ru(2)	2.794 (1)	Ru(1)–Ru(3)	2.938 (1)
Ru(2)–Ru(3)	2.779 (1)	Ru(1)–P(1)	2.320 (2)
Ru(2)–P(1)	2.251 (2)	Ru(1)–P(2)	2.314 (2)
Ru(3)–P(2)	2.378 (2)	Ru(1)–C(8)	2.138 (8)
Ru(2)–C(8)	2.313 (8)	Ru(2)–C(9)	2.374 (8)
Ru(3)–C(9)	2.116 (8)		
Angles			
Ru(1)–P(1)–Ru(2)	75.3 (1)	Ru(1)–P(2)–Ru(3)	77.5 (1)
Ru(1)–C(8)–Ru(2)	77.7 (3)	Ru(2)–C(9)–Ru(3)	76.2 (2)
Ru(1)–C(8)–C(9)	111.1 (5)	Ru(2)–C(8)–C(9)	74.7 (5)
Ru(2)–C(9)–C(8)	70.0 (5)	Ru(3)–C(9)–C(8)	110.6 (5)

**Table X. Selected Bond Lengths (Å) and Angles (deg) for 7**

Distances			
Ru(1)–Ru(2)	3.037 (2)	Ru(1)–Ru(3)	2.874 (2)
Ru(2)–Ru(3)	2.692 (2)	Ru(1)–P(1)	2.366 (4)
Ru(2)–P(2)	2.306 (5)	Ru(2)–C(9)	2.45 (2)
Ru(3)–C(9)	2.14 (2)	Ru(2)–Fe(1)	3.098 (3)
Angles			
Ru(1)–P(1)–C(13)	110.4 (5)	Ru(2)–C(9)–Ru(3)	71.5 (5)
Ru(2)–C(9)–C(13)	113 (1)	Ru(3)–C(9)–C(13)	124 (1)

data are summarized in Table I.

The structures were solved in each case by direct methods with the use of the EES routine in SHELX.<sup>34</sup> Hydrogen atoms were included in the models for **5–7** at their calculated positions (C–H = 0.97 Å). A weighting scheme,  $w = k/[\sigma^2(F) + gF^2]$ , was included, and the refinements were continued until convergence. No special features were noted from the analysis of variance for **5–7**, which indicated an appropriate weighting scheme had been applied in each case. The refinement of **8** was hindered owing to disorder of the heavy-atom positions. The structure analysis does, however, provide reliable information on the molecular structure. Refinement details are listed in Table I.

Scattering factors for neutral Ru and Fe (corrected for  $f'$  and  $f''$ ) were from ref 35, and values for the remaining atoms were

(34) Programs used included the following: ABSORB and SUSCAD, data reduction programs for CAD4 diffractometer, J. M. Guss, University of Sydney, 1976; PREABS and PROCES, data reduction programs for CAD4 diffractometer, University of Melbourne, 1981; SHELX, program for crystal structure determination, G. M. Sheldrick, University of Cambridge, 1976; ORTEP, Report ORNL-3994, C. K. Johnson, Oak Ridge National Laboratory, Oak Ridge, TN.

(35) Ibers, J. A., Hamilton, W. C., Eds. *International Tables for X-Ray Crystallography*; Kynoch Press: Birmingham, England, 1974; Vol. 4, pp 99, 149.

**Table XI. Selected Bond Lengths (Å) and Angles (deg) for 8**

Distances			
Ru(1)–Ru(2)	2.879 (2)	Ru(1)–Ru(3)	2.841 (4)
Ru(2)–Ru(4)	2.993 (4)	Ru(3)–Ru(4)	2.897 (3)
Ru(1)–P(1)	2.495 (7)	Ru(2)–P(1)	2.351 (7)
Ru(3)–P(1)	2.478 (7)	Ru(4)–P(1)	2.348 (7)
Ru(1)–C(1)	2.30 (3)	Ru(2)–C(1)	2.10 (3)
Ru(3)–C(2)	2.32 (3)	Ru(4)–C(2)	2.10 (2)
Ru(1)–C(9)	2.01 (3)	Ru(3)–C(9)	1.99 (3)
Angles			
Ru(1)–C(1)–Ru(2)	81.4 (9)	Ru(1)–C(1)–C(2)	108 (2)
Ru(2)–C(1)–C(2)	110 (2)	Ru(3)–C(2)–Ru(4)	81.8 (8)
Ru(3)–C(2)–C(1)	107 (2)	Ru(4)–C(2)–C(1)	113 (2)
Ru(1)–C(9)–Ru(3)	90 (1)		

those incorporated in SHELX.<sup>34</sup> Data solution and refinement were performed with the SHELX program system on the University of Adelaide's VAX11/780 computer system.

Atomic positions for the complexes 4–8 are given in Tables

II–VI and selected bond distances and angles in Tables VII–XI.

**Acknowledgment.** Financial support from the Natural Sciences and Engineering Research Council (W.R.C.) and the Australian Research Grants Scheme (M.I.B., M.R.S.) is gratefully acknowledged, as is an NSERC Exchange for M.I.B. and NSERC International Exchange Awards for W.R.C. O.b.S. thanks the Universiti Sains Malaysia for a Fellowship under the Academic Staff Training scheme.

**Registry No.** 3, 129521-33-1; 4, 129521-34-2; 5, 129521-35-3; 6, 129521-36-4; 7, 129521-37-5; 8, 129521-38-6.

**Supplementary Material Available:** Tables of bond lengths and angles and thermal parameters for complexes 4–8, together with tables of H atom positions and thermal parameters for compounds 5–7 (27 pages); listings of observed and calculated structure factors for complexes 4–8 (94 pages). Ordering information is given on any current masthead page.

## Early-Transition-Metal Ketenimine Complexes. Synthesis, Reactivity, and Structural Characterization of Complexes with $\eta^2(\text{C},\text{N})$ -Ketenimine Groups Bound to the Halogenobis((trimethylsilyl)cyclopentadienyl)niobium Unit.

### X-ray Structure of $\text{Nb}(\eta^5\text{-C}_5\text{H}_4\text{SiMe}_3)_2\text{Cl}(\eta^2(\text{C},\text{N})\text{-PhN}=\text{C}=\text{CPh}_2)$

Antonio Antiñolo,<sup>†</sup> Mariano Fajardo,<sup>†</sup> Carmen López Mardomingo,<sup>‡</sup> and Antonio Otero<sup>\*†</sup>

*Departamento de Química Inorgánica and Departamento de Química Orgánica, Campus Universitario, Universidad de Alcalá de Henares, 28871 Alcalá de Henares, Spain*

Youssef Mourad and Yves Mugnier

*Laboratoire de Synthèse et d'Electrosynthèse Organometalliques associé au CNRS (UA 33), Faculté des Sciences, 6 Bd. Gabriel, 21000 Dijon, France*

Julia Sanz-Aparicio, Isabel Fonseca, and Feliciano Florencio

*UEI de Cristalografía, Instituto Rocasolano, CSIC, Serrano 119, 28006 Madrid, Spain*

Received January 5, 1990

The reaction of  $\text{Nb}(\eta^5\text{-C}_5\text{H}_4\text{SiMe}_3)_2\text{X}$  ( $\text{X} = \text{Cl}, \text{Br}$ ) with 1 equiv of various ketenimines,  $\text{R}^1\text{N}=\text{C}=\text{CR}^2\text{R}^3$ , leads to the niobium derivatives  $\text{Nb}(\eta^5\text{-C}_5\text{H}_4\text{SiMe}_3)_2\text{X}(\eta^2(\text{C},\text{N})\text{-R}^1\text{N}=\text{C}=\text{CR}^2\text{R}^3)$  (1,  $\text{X} = \text{Cl}$ ,  $\text{R}^1 = \text{R}^2 = \text{R}^3 = \text{C}_6\text{H}_5$ ; 2,  $\text{X} = \text{Cl}$ ,  $\text{R}^1 = p\text{-CH}_3\text{-C}_6\text{H}_4$ ,  $\text{R}^2 = \text{R}^3 = \text{C}_6\text{H}_5$ ; 3,  $\text{X} = \text{Br}$ ,  $\text{R}^1 = \text{R}^2 = \text{R}^3 = \text{C}_6\text{H}_5$ ; 4,  $\text{X} = \text{Br}$ ,  $\text{R}^1 = p\text{-CH}_3\text{-C}_6\text{H}_4$ ,  $\text{R}^2 = \text{R}^3 = \text{C}_6\text{H}_5$ ; 5,  $\text{X} = \text{Cl}$ ,  $\text{R}^1 = \text{R}^2 = \text{C}_6\text{H}_5$ ,  $\text{R}^3 = \text{CH}_3$ ; 6,  $\text{X} = \text{Br}$ ,  $\text{R}^1 = \text{R}^2 = \text{C}_6\text{H}_5$ ,  $\text{R}^3 = \text{CH}_3$ ) with the expected ketenimine  $\text{C}=\text{N}$  bonding mode. Reduction of 1 with 1 equiv of  $\text{Na}/\text{Hg}$  gives the complex  $\text{Nb}(\eta^5\text{-C}_5\text{H}_4\text{SiMe}_3)_2(\eta^2(\text{C},\text{N})\text{-PhN}=\text{C}=\text{CPh}_2)$  (9) as a paramagnetic compound. The reduction of 9 with 1 equiv of  $\text{Na}/\text{Hg}$  and the subsequent addition of a proton source (ethanol) leads to the iminoacyl compound  $\text{Nb}(\eta^5\text{-C}_5\text{H}_4\text{SiMe}_3)_2(\text{CRNR}^1)$  (10,  $\text{R} = \text{CH}(\text{Ph}_2)$ ,  $\text{R}^1 = \text{Ph}$ ). The one- and two-electron reductions of 1 have been studied by cyclic voltammetry experiments. The structure of 1 was determined by single-crystal X-ray diffractometry:  $a = 24.4904$  (14) Å,  $b = 11.0435$  (04) Å,  $c = 26.6130$  (15) Å,  $\beta = 109.890$  (5)°, monoclinic, space group  $C2/c$ ,  $Z = 8$ ,  $V = 6768.4$  (5) Å<sup>3</sup>,  $\rho_{\text{calcd}} = 1.3194$  g/mL,  $R = 0.048$ ,  $R_w = 0.060$  based on 4806 observed reflections. The structure contains a niobium atom bonded to two cyclopentadienyl rings in a  $\eta^5$  fashion; the coordination of the metal is completed by a Cl atom and a  $\eta^2(\text{C},\text{N})$ -bonded ketenimine ligand.

### Introduction

The preparative usefulness of organometallic complexes as new reagents in organic syntheses has been increasing

in the recent years.<sup>1</sup> Ketenes, ketenimines, and related heterocumulenes are very reactive organic molecules whose typical reactivity patterns are well-defined.<sup>2</sup> Several

<sup>†</sup> Departamento de Química Inorgánica.

<sup>‡</sup> Departamento de Química Orgánica.

(1) Collman, J. P.; Hegedus, L. S.; Norton, J. R.; Finke, R. G. *Principles and Applications of Organotransition Metal Chemistry*; University Science Books: Mill Valley, CA, 1987; Vol. III, p 669.